

# A characteristic length scale for density gradients in supercritical monocomponent flows near pseudoboiling

By L. Jofre† AND J. Urzay

## 1. Motivation and objectives

At pressures  $P$  moderately larger than the critical value  $P_c$ , it is known that pure substances behave differently depending on whether their temperature  $T$  is larger or smaller than a characteristic value  $T_{pb}$  referred to as the pseudoboiling temperature, which increases with pressure, as shown in Figure 1(a). The pseudoboiling temperature is typically defined as the temperature at which the specific heat at constant pressure  $c_p$  reaches a finite local maximum, which is reminiscent of a phase transition of second kind. In particular, at sub-pseudoboiling temperatures  $T < T_{pb}$ , pure substances behave as liquid-like supercritical fluids: (a) their density  $\rho$  is large; (b) their isothermal compressibility  $\beta_T = (1/\rho)(\partial\rho/\partial P)_T$  is small; (c) their dynamic viscosity  $\mu$  and thermal conductivity  $\lambda$  decrease with temperature; and (d) their mass diffusivity  $D$  remains mostly constant or increases slowly with temperature. In contrast, at super-pseudoboiling temperatures  $T > T_{pb}$ , pure substances behave as gas-like supercritical fluids: (a) their  $\rho$  is relatively smaller; (b) their  $\beta_T$  is relatively larger; and (c) their  $\mu$ ,  $\lambda$ , and  $D$  increase with temperature (Poling *et al.* 2001).

In many instances, the transition from liquid-like to gas-like supercritical states across the pseudoboiling line has been referred to as transcritical in monocomponent systems. Of particular interest in this transition are the resulting large density variations with respect to temperature. For instance, in the density distributions shown in Figure 1(b) for  $N_2$ , the liquid-like to gas-like supercritical density ratio between the temperatures  $T_1 = 0.5T_c$  and  $T_2 = 7T_c$  at  $P = 2P_c$  ( $T_c = 126$  K,  $P_c = 34$  bar) is approximately 34. These density variations are maximum near pseudoboiling (Maxim *et al.* 2019). This is shown in Figure 1(c) by the concurrent spike in volume expansivity  $\beta_v = -(1/\rho)(\partial\rho/\partial T)_P$ .

In this report, the characteristic length  $\delta_\rho$  associated with the density gradients across the pseudoboiling line is estimated for laminar and turbulent monocomponent mixing layers consisting of a supercritical stream injected at velocity  $U_1$  and temperature  $T_1 < T_{pb}$  into a supercritical environment at velocity  $U_2 < U_1$  and temperature  $T_2 > T_{pb}$ , as sketched in Figure 2(a). It is shown below that  $\delta_\rho$  is an increasing fraction of the mixing-layer thickness  $\delta_M$  as the pressure increases.

## 2. The characteristic length scale $\delta_\rho$

The dimensionless density variations across the pseudoboiling temperature are of order

$$\Delta\rho_{pb}/\rho_{pb} \sim \beta_{v,pb}\Delta T_{pb}, \quad (2.1)$$

with  $\rho_{pb}$  and  $\beta_{v,pb}$  being the density and volume expansivity at pseudoboiling, respectively. An approximate way of characterizing the temperature variations across the pseu-

† Presently at UPC - BarcelonaTech, Spain.

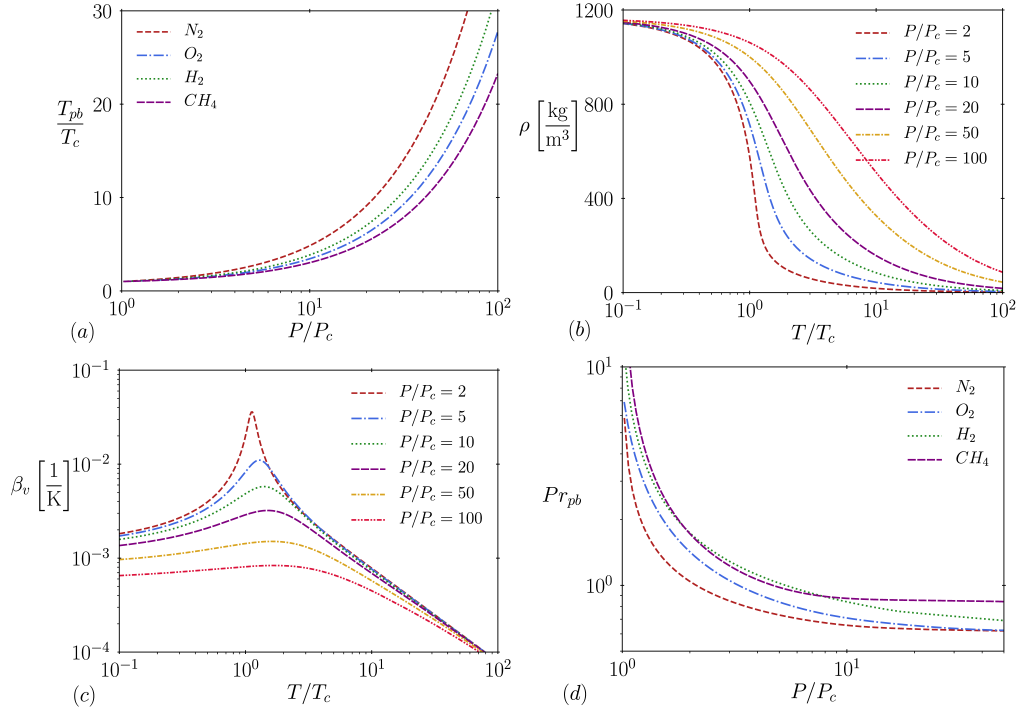


FIGURE 1. (a) Reduced pseudoboiling temperature  $T_{pb}/T_c$  as a function of the reduced pressure  $P/P_c$  for  $N_2$ ,  $O_2$ ,  $H_2$ , and  $CH_4$ . (b) Density of  $N_2$  as a function of the reduced temperature  $T/T_c$  at different pressures. (c) Volume expansivity  $\beta_v$  of  $N_2$  as a function of reduced temperature  $T/T_c$  at different pressures. (d) Prandtl number at pseudoboiling  $Pr_{pb}$  as a function of the reduced pressure  $P/P_c$  for  $N_2$ ,  $O_2$ ,  $H_2$  and  $CH_4$ . The reader is referred to Jofre & Urzay (2021) for the formulation employed to calculate these quantities.

doboiling line,  $\Delta T_{pb}$ , is by associating them with the characteristic width of the volume-expansivity peak around pseudoboiling in temperature space as

$$\Delta T_{pb} = \frac{1}{\beta_{v,pb}} \int_{T_1}^{T_2} \beta_v dT. \quad (2.2)$$

With Eqs. (2.1) and (2.2) in mind, the estimation of  $\delta_\rho$  is described below for laminar mixing layers followed by the more difficult case of turbulent mixing layers. The analysis can be easily extended to other cases like turbulent wall-bounded flows of practical interest for regenerative cooling of rocket engines. Such extensions are not attempted here for the sake of maintaining a fast pace of exposition of the basic concepts.

### 2.1. Laminar flow

Consider the sketch in Figure 2(a). The temperature gradients across the mixing layer can be estimated as  $\partial T/\partial y \sim (T_2 - T_1)/\delta_T$ , with  $\delta_T \sim \delta_M/\sqrt{Pr_{pb}}$  the thermal mixing-layer thickness. In this notation,  $Pr_{pb}$  represents the Prandtl number evaluated at pseudoboiling, which is plotted in Figure 1(d) as a function of pressure. Since the temperature gradient is continuous across the pseudoboiling line, it can also be estimated as  $\partial T/\partial y \sim \Delta T_{pb}/\delta_\rho$ . As a result, the ratio of the characteristic length associated with the

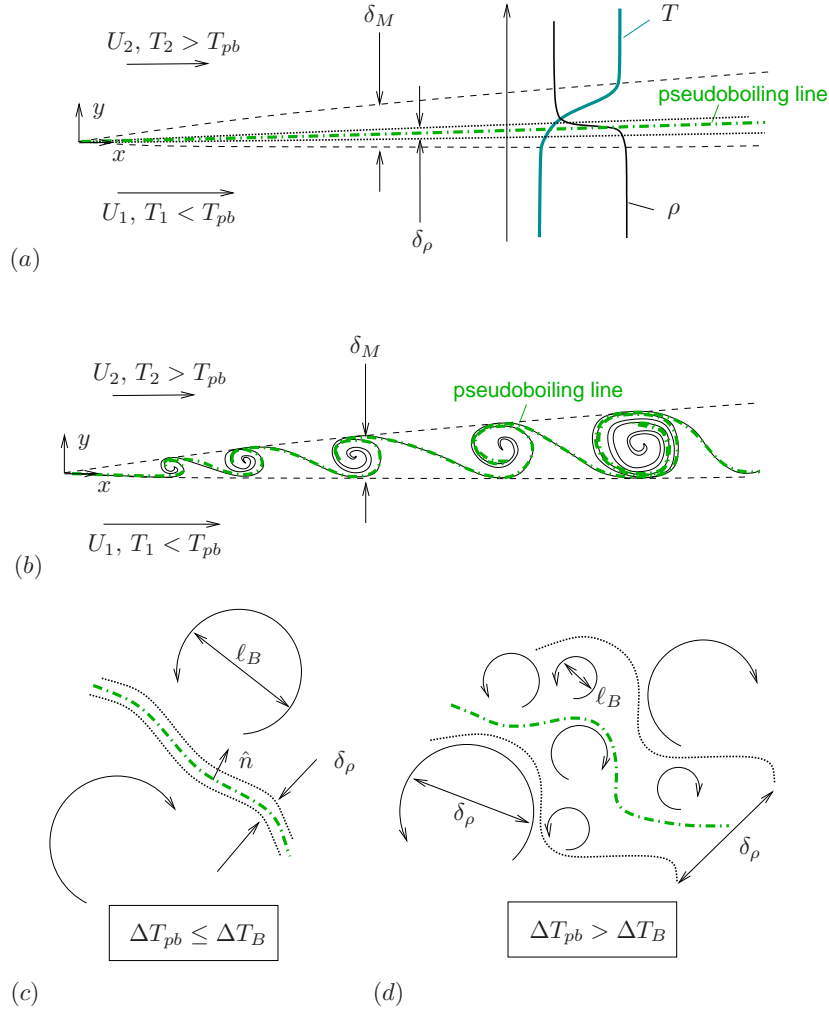


FIGURE 2. Schematics of (a) laminar and (b) turbulent mixing layers arising when a supercritical stream is injected at sub-pseudoboiling temperature into a supercritical environment of the same component at super-pseudoboiling temperature. Panels (c) and (d) represent two distinguished turbulent cases analyzed in the text.

density gradients near pseudoboiling and the laminar mixing-layer thickness is of order

$$\frac{\delta_\rho}{\delta_M} \sim \frac{\Delta T_{pb}}{(T_2 - T_1)\sqrt{Pr_{pb}}}, \quad (2.3)$$

with  $\Delta T_{pb}$  being calculated using Eq. (2.2). As shown in Figure 3,  $\delta_\rho$  is a fraction of  $\delta_M$  smaller than 10% near the critical pressure at  $P/P_c \approx 2$ . This fraction increases monotonically with pressure, reaching values of order unity for  $P/P_c = O(10^3)$  in all cases. Also implied by Eq. (2.3) is that the increase in  $\delta_\rho$  with downstream distance  $x$  occurs approximately at the same rate as that of  $\delta_M$  predicted by boundary-layer theory.

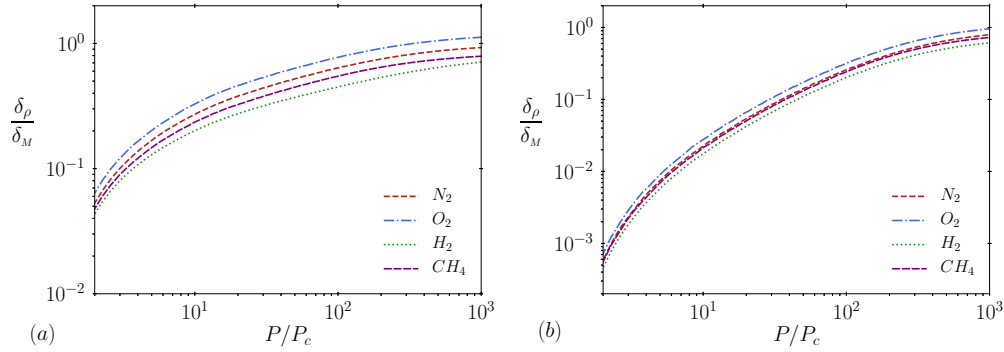


FIGURE 3. (a) Eq. (2.3) and (b) Eq. (2.5) evaluated as a function of reduced pressure  $P/P_c$  for  $N_2$ ,  $O_2$ ,  $H_2$ , and  $CH_4$  with injection temperatures  $T_1 = 0.5T_{pb}$  and  $T_2 = 10T_{pb}$ .

## 2.2. Turbulent flow

Consider the sketch in Figure 2(b). In turbulent flows, the Batchelor length  $\ell_B$  represents the microscale for the temperature and is related to the Kolmogorov length  $\ell_k = (\nu_{pb}^3/\epsilon)^{1/4}$  as  $\ell_B \sim \ell_k/\sqrt{Pr_{pb}}$ , where  $\nu_{pb}$  is the kinematic viscosity at pseudoboiling and  $\epsilon$  is an average turbulent dissipation rate in the mixing layer. Assuming an invariance of the temperature scalar dissipation rate across the inertial subrange, the characteristic fluctuation of the temperature at the Batchelor scale can be estimated as  $\Delta T_B \sim (T_2 - T_1)/Re_M^{1/4}$ , where  $Re_M = (U_1 - U_2)\delta_M/\nu_{pb}$  is the Reynolds number of the large-scale relative motion in the mixing layer. In performing this estimate, it has been assumed that the integral scale is of order  $\delta_M$  and is subjected to temperature and velocity fluctuations of order  $T_2 - T_1$  and  $U_1 - U_2$ , respectively. Two cases arise depending on the value of  $\Delta T_B$  relative to  $\Delta T_{pb}$ , the latter being independently given by the thermodynamic properties of the pure substance and computed using Eq. (2.2) at the corresponding operating pressure.

In the first case, the temperature fluctuations across the Batchelor length are larger than  $\Delta T_{pb}$ , namely  $\Delta T_B/\Delta T_{pb} \gtrsim 1$ , as sketched in Figure 2(c). In this case, the density gradients are embedded in the smallest scales of turbulence. This requires moderately high Reynolds numbers satisfying both  $Re_M \leq [(T_2 - T_1)/\Delta T_{pb}]^4$  and  $Re_M \gg 1$ . The corresponding temperature gradients across the pseudoboiling line can be estimated as  $\partial T/\partial \hat{n} \sim \Delta T_B/\ell_B \sim \Delta T_{pb}/\delta_\rho$  because they are maximum at the Batchelor scale. As a result, the ratio of the characteristic length associated with the density gradients near pseudoboiling and the Kolmogorov length is

$$\frac{\delta_\rho}{\ell_k} \sim \frac{\Delta T_{pb}}{(T_2 - T_1)\sqrt{Pr_{pb}}} Re_M^{1/4}. \quad (2.4)$$

In Eq. (2.4), the prefactor multiplying  $Re_M^{1/4}$  corresponds to the right-hand side of Eq. (2.3) plotted in Figure 3, or equivalently, to the ratio between  $\delta_\rho$  and the mixing-layer thickness  $\delta_M$  in the laminar case. Since  $Re_M^{1/4}$  is most likely not a too large parameter in practical applications in this regime, the results presented in Figure 3(a) could also be interpreted approximately as the ratio  $\delta_\rho/\ell_k$  in this case, thereby indicating that  $\delta_\rho$  is an increasing fraction of the Kolmogorov length with increasing pressure above the critical point. Instead, if  $Re_M^{1/4}$  is a large parameter in the desired operating conditions, then Figure 3(a) provides  $Re_M^{-1/4}\delta_\rho/\ell_k$  as a function of the reduced pressure.

In the second case, the temperature fluctuations across the Batchelor scale are larger than  $\Delta T_{pb}$ , namely  $\Delta T_B/\Delta T_{pb} < 1$ , as sketched in Figure 2(d). This requires sufficiently high Reynolds numbers satisfying both  $Re_M > [(T_2 - T_1)/\Delta T_{pb}]^4$  and  $Re_M \gg 1$ . In this case, the small eddies can penetrate and broaden the zone around the pseudoboiling line where the density is rapidly varying. By assuming an invariance of both the temperature scalar dissipation rate and turbulent dissipation rate in the inertial subrange, the temperature fluctuations of the eddies of size similar to  $\delta_\rho$  are related to the temperature fluctuations of the large eddies as  $\epsilon^{1/3}(\Delta T_{pb})^2/\delta_\rho^{2/3} \sim \epsilon^{1/3}(T_2 - T_1)^2/\delta_M^{2/3}$ . As a result, the ratio of  $\delta_\rho$  to the turbulent mixing-layer thickness  $\delta_M$  can be estimated as

$$\frac{\delta_\rho}{\delta_M} \sim \left( \frac{\Delta T_{pb}}{T_2 - T_1} \right)^3. \tag{2.5}$$

Equivalently, Eq. (2.5) can be expressed as

$$\frac{\delta_\rho}{\ell_k} \sim \left( \frac{\Delta T_{pb}}{T_2 - T_1} \right)^3 Re_M^{3/4} \tag{2.6}$$

in terms of the Kolmogorov length  $\ell_k$ . The ratio (2.5) is provided in Figure 3(b) as a function of pressure. Because of the higher Reynolds numbers involved, a much smaller ratio  $\delta_\rho/\delta_M$  occurs in the turbulent case relative to the laminar one. Specifically, near the critical point,  $P/P_c \approx 2$ , Figure 3(b) indicates that  $\delta_\rho$  is a fraction of order 0.01% – 0.1% of the turbulent mixing-layer thickness  $\delta_M$ .

### 3. Concluding remarks

Simple estimates have been provided in this report for the characteristic length  $\delta_\rho$  associated with density gradients across the pseudoboiling line in monocomponent supercritical mixing layers. Equation (2.3) is appropriate for laminar mixing layers. Equation (2.4) is appropriate for turbulent mixing layers at moderately high Reynolds numbers such that the temperature fluctuations across the Batchelor scale are larger than the temperature variations across the pseudoboiling line. Equations (2.5) or (2.6) are appropriate for turbulent mixing layers at high Reynolds numbers such that the temperature fluctuations across the Batchelor scale are smaller than the temperature variations across the pseudoboiling line. The results obtained here indicate that the characteristic length  $\delta_\rho$  increases with pressure and becomes of the same order as the characteristic length of the large-scale features of the flow only at elevated pressures of order  $10^3 P_c$ . However, a number of approximations have been made in order to perform these estimates that may be not be entirely justifiable in turbulent mixing layers. Amongst them, the reader should be particularly cautious about the assumption of an isotropic forward cascade unaffected by density variations.

In order to infer estimates of the density gradient  $\Delta\rho_{pb}/\delta_\rho$ , a readout of  $\delta_\rho$  from Figure 3 should be accompanied by a readout of the corresponding nondimensional density variations  $\Delta\rho_{pb}/\rho_{pb}$  from Figure 4, with  $\rho_{pb}$  calculated from the equation of state using the pressure and pseudoboiling temperature in Figure 1(a). Since  $\delta_\rho$  increases with pressure, and  $\Delta\rho_{pb}$  decreases with pressure, the density gradients become increasingly less dynamically relevant the farther the pressure is above the critical pressure. Specifically, as the pressure increases, the maximum of  $c_p$  becomes increasingly less pronounced, the pseudoboiling line fades away, and the pure substance increasingly resembles a fully supercritical one of uniform thermodynamic response over the entire temperature range.

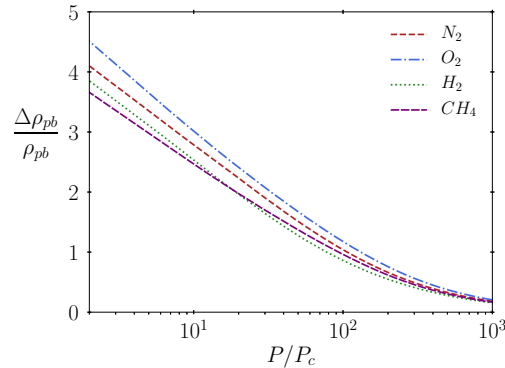


FIGURE 4. Non-dimensional density variations  $\Delta\rho_{pb}/\rho_{pb}$  across the pseudoboiling line estimated using Eqs. (2.1)-(2.2) evaluated as a function of the reduced pressure  $P/P_c$  for  $N_2$ ,  $O_2$ ,  $H_2$ , and  $CH_4$  with injection temperatures  $T_1 = 0.5T_{pb}$  and  $T_2 = 10T_{pb}$ .

It is worth emphasizing that the density gradients analyzed here for supercritical monocomponent flows near pseudoboiling are fundamentally different from the interfaces arising in subcritical monocomponent flows and in transcritical bicomponent flows. In particular, supercritical monocomponent systems are thermodynamically stable, and therefore cannot engender any interfaces. As a result, these density gradients do not bear any surface tension, or equivalently, are not subjected to any local excess of potential energy. Instead, their characteristic length  $\delta_\rho$  is always a fraction of the hydrodynamic scale associated with the rate of heat conduction across the pseudoboiling isotherm. This is in contrast to the interfaces that emerge as a result of thermodynamic instabilities in subcritical monocomponent systems and transcritical bicomponent systems. In particular, those interfaces are endowed with surface tension, and their thicknesses are largely independent of the surrounding hydrodynamic scales (Jofre & Urzay 2021).

### Acknowledgments

The authors are grateful to Dr. Kazuki Maeda for raising the question of how to estimate  $\delta_\rho$  during a CTR Tea Seminar that the second author gave in Fall 2020 on a related topic. The second author was funded by the Advanced Simulation and Computing (ASC) program of the U.S. Department of Energy's National Nuclear Security Administration (NNSA) via the PSAAP-III Center at Stanford, grant # DE-NA0003968.

### REFERENCES

- POLING, B. E., PRAUSNITZ, J. M. & O'CONNELL, J. P. 2001 *The Properties of Gases and Liquids*. McGraw-Hill.
- MAXIM, F., CONTESCU, C., BOILLAT, P., NICENO, B., KARALIS, K., TESTINO, A. & LUDWIG, C. 2019 Visualization of supercritical water pseudo-boiling at Widom line crossover. *Nat. Comm.* **10**, 4114.
- JOFRE, L. & URZAY, J. 2021 Transcritical diffuse-interface hydrodynamics of propellants in high-pressure combustors of chemical propulsion systems. *Prog. Ener. Combust. Sci.* **82**, 100877.